residues of the Ncd neck by our definition (*5*) and NcdKHC6 lacks four residues of the KHC neck according to the dimer KHC crystal structure in which the coiled coil begins four residues COOH-terminal to the start of the heptad repeats (*8*). The hybrid proteins also differ in that NcdKHC6 has the Ncd stalk at the NH_2-terminus of the motor, joined to the Ncd neck, whereas ncd-Nkin has the KHC stalk at the COOH-terminus, joined to the KHC neck (Fig. 1). Strikingly, NcdKHC6 is a minus-end motor and ncd-Nkin is a plus-end motor (*2*). Thus an intact neck, or the attachment of the neck to the stalk, may be important for motor polarity rather than simply the neck and neck-motor junction.

The NcdKHC1 motor was slow compared with Ncd (Table 1), suggesting that the neck-motor junction, or another aspect of the coupling of the motor to the stalk and neck, is imperfect. NcdKHC2 and NcdKHC5 were even slower than NcdKHC1, suggesting that the Ncd neck or neck-motor junction may affect motor velocity. The neck of myosin, a molecular motor with structural similarity to kinesin and Ncd (*4*), has been shown to contribute to motor velocity (*14*), although the effects of the myosin and Ncd necks on motor velocity may differ. Our results indicate that polarity determinants, residues or regions that contribute to the direction of motor movement, are present in the Ncd neck and the KHC motor core. Neck residues immediately adjacent to the conserved motor core are critical for Ncd minus-end movement and attachment to the stalk may also be important.

References and Notes

1. G. S. Bloom and S. A. Endow, *Protein Profile* **2**, 1109 (1995); R. D. Vale, *J. Cell Biol.* **135**, 291 (1996); N. Hirokawa, *Science* **279**, 519 (1998).
2. U. Henningsen and M. Schliwa, *Nature* **389**, 93 (1997).
3. R. B. Case, D. W. Pierce, N. Hom-Booher, C. L. Hart, R. D. Vale, *Cell* **90**, 959 (1997).
4. E. P. Sablin, F. J. Kull, R. Cooke, R. D. Vale, R. J. Fletterick, *Nature* **380**, 555 (1996); F. J. Kull, E. P. Sablin, R. Lau, R. J. Fletterick, R. D. Vale, *ibid.*, p. 550.
5. S. A. Endow and R. J. Fletterick, *Bioessays* **20**, 108 (1998).
6. A. Lupas and M. Van Dyke, J. Stock, *Science* **252**, 1162 (1991).
7. I. M.-T. C. Crevel, A. Lockhart, R. A. Cross, *J. Mol. Biol.* **273**, 160 (1997); R. D. Vale and R. J. Fletterick, *Annu. Rev. Cell Dev. Biol.* **13**, 745 (1997); L. Romberg, D. W. Pierce, R. D. Vale, *J. Cell Biol.* **140**, 1407 (1998).
8. F. Kozielski *et al.*, *Cell* **91**, 985 (1997).
9. NcdKHC1 consists of glutathione S-transferase (GST) fused to the Ncd stalk and neck followed by the *Drosophila* KHC motor core and the Ncd COOH-terminus [residues 664 to 700 that extend beyond the conserved motor core and may interact with the Ncd neck (*4*)]. NcdKHC2–5 are mutants of NcdKHC1 (Fig. 1). NcdKHC6 consists of the Ncd stalk, neck, and motor with the Ncd COOH-terminus replaced by the *Drosophila* KHC neck.
10. The *pGEX/ncdkhc1–5* chimeric plasmids were constructed from a plasmid coding for GST fused to Ncd residues 194 to 346 [S. A. Endow, S. Henikoff, L. Soler-Niedziela, *Nature* **345**, 81 (1990)], followed by *Drosophila* KHC residues 11 to 340 [J. T. Yang, R. A. Laymon, L. S. B. Goldstein, *Cell* **56**, 879 (1989)]. The plasmid was constructed by using the polymerase chain reaction (PCR) and wild-type *ncd* and *khc* plasmids [H. Song and S. A. Endow, *Biochemistry* **35**, 11203 (1996)]. A Bam HI site was created to ligate *ncd* to *pGEX-2T* [D. B. Smith and K. S. Johnson, *Gene* **67**, 31 (1988)] and a Bss HII site was created for the junction with *khc*, chosen because it minimally altered the Ncd neck according to the computer program COILS (*6*), changing L345A. The *khc* primers contained a Bss HII site, sequences coding for residues 338 to 340 missing from the *khc* plasmid, and an Eco RI site for ligation to *pGEX-2T*. *pGEX/ncdkhc2* and *-3* were made by replacing the Nsi I–Eco RI fragment of the plasmid with overlap extension PCR fragments [S. N. Ho, H. D. Hunt, R. M. Horton, J. K. Pullen, L. R. Pease, *Gene* **77**, 51 (1989)] to substitute Ncd residues 664 to 700 for KHC residues 327 to 340 or to delete KHC after residue 326 and add a glycine. *pGEX/ncdkhc1*, *-4*, and *-5* were made from *pGEX/ncdkhc2* by replacing the Sph I–Nsi I fragment with overlap PCR fragments that repaired the L345A mutation in the Ncd neck or shifted the neck-motor junction by two residues or both. *pGEX/ncdkhc6* was made from *pGEX/MC1* (*13*) and wild-type *khc* by replacing the *pGEX/MC1* Bst EII–Eco RI fragment with an overlap PCR fragment coding for Ncd to residue 663, followed by KHC residues 327 to 340. All plasmids were sequenced to confirm the intended changes and exclude PCR mutations.
11. The chimeric plasmids were transformed into *BL21(DE3)pLysS* cells for protein expression [F. W. Studier, A. H. Rosenberg, J. J. Dunn, J. W. Dubendorff, *Methods Enzymol.* **185**, 60 (1990)]. Cells were grown in M9ZB to an OD_{550} of 0.65 to 1 and induced at 21° to 22°C. Induction times, usually 5 to 6 hours, were optimized by analysis on polyacrylamide gels. The molecular weight of the major induced protein band in each case corresponded to the predicted molecular weight of the hybrid protein. Lysates for motility assays were prepared as described in (*15*). Microtubule gliding assays were carried out by video-enhanced differential interference contrast (VE-DIC) microscopy [R. A. Walker *et al.*, *J. Cell Biol.* **107**, 1437 (1988)]. Samples of cell lysates used in motility experiments were analyzed on immunoblots. Proteins were reacted with antibody to HIPER, directed against a highly conserved sequence motif in the kinesin motor domain [K. E. Sawin, T. J. Mitchison, L. G. Wordeman, *J. Cell Sci.* **101**, 303 (1992)] (gift of K. Sawin, ICRF, London) or an antibody to Ncd COOH-terminus residues 670 to 682 [M. Hatsumi and S. A. Endow, *J. Cell Sci.* **103**, 1013 (1992)] and detected with an alkaline phosphatase system. A single major band of the predicted molecular weight was observed in each case, indicating that the chimeric proteins in the lysates used for the motility assays were intact.
12. Axoneme-microtubule complexes were prepared as described in (*15*). To determine gliding velocities, we tracked axoneme-microtubule complexes with a custom tracking program (a gift of N. Gliksman and T. Salmon, University of North Carolina, Chapel Hill, NC).
13. R. Chandra, E. D. Salmon, H. P. Erickson, A. Lockhart, S. A. Endow, *J. Biol. Chem.* **268**, 9005 (1993).
14. T. Q. P. Uyeda, P. D. Abramson, J. A. Spudich, *Proc. Natl. Acad. Sci. U.S.A.* **93**, 4459 (1996).
15. H. Song, M. Golovkin, A. S. N. Reddy, S. A. Endow, *ibid.*, **94**, 322 (1997).

16. Supported by a grant from NIH. E. Sablin and R. Fletterick made valuable comments on constructs and motor structure. We thank H. Song for axonemes and for helpful comments on the manuscript.

9 April 1998; accepted 7 July 1998

Characterization of an Ammonium Transport Protein from the Peribacteroid Membrane of Soybean Nodules

Brent N. Kaiser, Patrick M. Finnegan, Stephen D. Tyerman, Lynne F. Whitehead, Fraser J. Bergersen, David A. Day,* Michael K. Udvardi

Nitrogen-fixing bacteroids in legume root nodules are surrounded by the plant-derived peribacteroid membrane, which controls nutrient transfer between the symbionts. A nodule complementary DNA (*GmSAT1*) encoding an ammonium transporter has been isolated from soybean. *GmSAT1* is preferentially transcribed in nodules and immunoblotting indicates that GmSAT1 is located on the peribacteroid membrane. [^{14}C]methylammonium uptake and patch-clamp analysis of yeast expressing GmSAT1 demonstrated that it shares properties with a soybean peribacteroid membrane NH_4^+ channel described elsewhere. GmSAT1 is likely to be involved in the transfer of fixed nitrogen from the bacteroid to the host.

Many legumes form a symbiotic relationship with N_2-fixing bacteria called rhizobia, which enables the plants to grow on soils depleted of combined nitrogen. Differentiated rhizobia, called bacteroids, are housed in specialized organs (nodules) on the legume roots. Within the infected cells of nodules, N_2-fixing bacteroids are enclosed by the plant-derived peribacteroid membrane (PBM), which segregates the bacteroids from the plant cytosol and controls nutrient exchange between the symbionts. The organelle-like structure consisting of PBM, bacteroid, and the intervening peribacteroid space (PBS) is known as the symbiosome (*1*). In soybean, NH_4^+ is probably the main form of nitrogen exported from the symbiosome (*2*) and analysis of PBM isolated from soybean and pea has identified a monovalent cation channel with

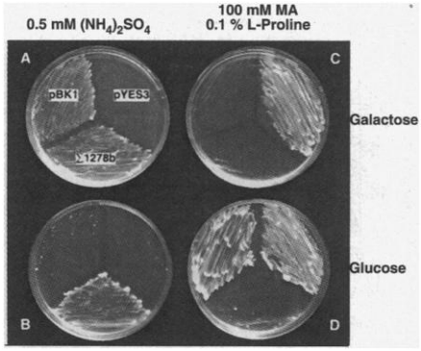

Fig. 1. Growth of mutant 26972c yeast cells transformed with either pBK1 or pYES3 and wild-type strain Σ1278b (*4*). Growth on minimal medium (*9*) containing 1 mM NH_4^+ and galactose at 10 mg ml^{-1} (**A**); 1 mM NH_4^+ and glucose at 10 mg ml^{-1} (**B**); 100 mM MA, 0.1% L-proline, and galactose at 10 mg ml^{-1} (**C**); and 100 mM MA, 0.1% L-proline, and glucose at 10 mg ml^{-1} (**D**).

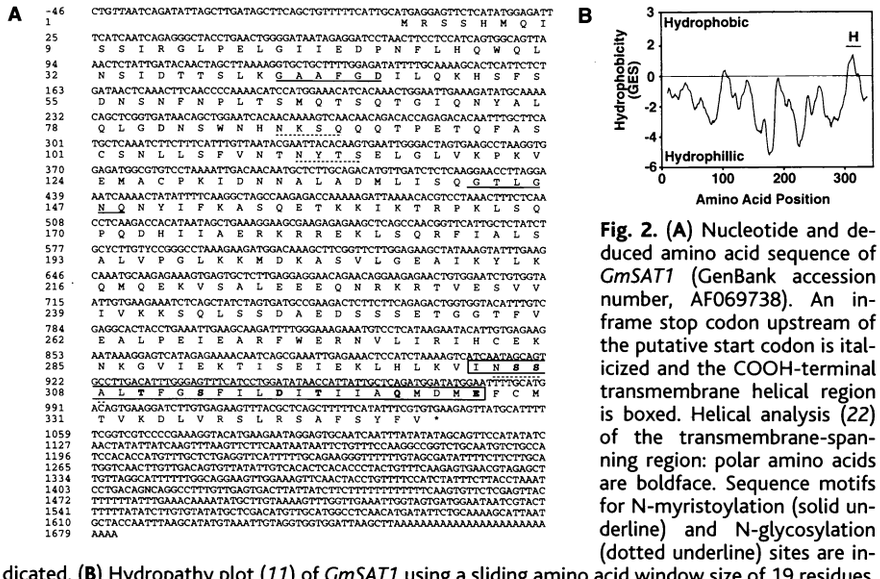

Fig. 2. (**A**) Nucleotide and deduced amino acid sequence of *GmSAT1* (GenBank accession number, AF069738). An in-frame stop codon upstream of the putative start codon is italicized and the COOH-terminal transmembrane helical region is boxed. Helical analysis (*22*) of the transmembrane-spanning region: polar amino acids are boldface. Sequence motifs for N-myristoylation (solid underline) and N-glycosylation (dotted underline) sites are indicated. (**B**) Hydropathy plot (*11*) of *GmSAT1* using a sliding amino acid window size of 19 residues. Horizontal bar indicates putative helical membrane-spanning region.

a preference for NH_4^+ (*3*). This channel is likely to be the main route for NH_4^+ flux to the plant.

We have used functional complementation of the *Saccharomyces cerevisiae* NH_4^+ transport mutant 26972c (*mep1 mep2 ura3*) to isolate a cDNA encoding a PBM NH_4^+ transporter. This yeast mutant lacks the high-affinity plasma membrane NH_4^+ transporters Mep1p and Mep2p and exhibits slow growth relative to the wild type in the presence of limiting (2 mM) NH_4^+ (*4*). This mutant has been used to isolate cDNAs encoding high-affinity NH_4^+ transporters from both *S. cerevisiae* (*5*) and *Arabidopsis thaliana* (*6*). Mutant 26972c was transformed with a cDNA library synthesized from 6-week-old soybean nodules (*7*). The cDNA was ligated in the sense orientation downstream of the galactose-inducible yeast *GAL1* promoter in the *URA3*-containing *Escherichia coli* yeast shuttle vector pYES3 (*8*). Transformants (URA^+) were initially screened for increased growth rate on medium containing 2 mM NH_4^+ plus galactose and for the slow-growth phenotype of the mutant in the presence of glucose, a repressor of the *GAL1* promoter (*9*). This strategy enabled the isolation of a plasmid (pBK1) containing a 1.7-kb cDNA that, when reintroduced into mutant 26972c, once again allowed growth on limiting NH_4^+ (Fig. 1).

The cDNA insert in pBK1 was sequenced (*10*) and found to encode a 348–amino acid protein with a predicted mass of 39,153 daltons (Fig. 2). The gene encoding this protein has been named *GmSAT1* (*Glycine max* symbiotic ammonium transport protein). Searches of databases for related gene or protein sequences failed to find significant extended sequence similarity between GmSAT1 and other known proteins. Analysis of the GmSAT1 sequence for specific motifs revealed two potential sites for N-myristoylation and three potential sites for N-glycosylation (Fig. 2A). Secondary structure analysis suggested that residues 178 to 217 encode a helix-loop-helix motif (Fig. 2A). Hydropathy analysis (*11*) identified one putative membrane-spanning helical region at the COOH-terminus (Fig. 2). Northern blot analysis of polyadenylated [poly$(A)^+$] RNA isolated from soybean tissues (*12*) indicated that the *GmSAT1* transcript is present at much greater levels in nodules than in any other organ of the plant (Fig. 3). Some *GmSAT1* mRNA was also detected in inoculated roots from which the nodules had been removed (Fig. 3, lane 2), suggesting that *GmSAT1* expression is triggered by a signal that diffuses from the nodule into root tissues. No transcript was detected in uninoculated roots (Fig. 3, lane 3), indicating that *GmSAT1* is symbiosis specific. Southern blot analysis of leaf DNA indicated that *GmSAT1* may be a member of a multigene family in soybean (*13*).

A truncated GmSAT1 protein, containing only the hydrophilic portion, was His-tagged and overexpressed in *E. coli* (*14*). After affinity purification, a polyclonal antiserum against the protein was raised in rabbit (*15*). The antiserum was used to probe immunoblots of total soluble and purified plasma membrane fractions prepared (*16*) from yeast mutant 26972c transformed with pYES3 or pBK1. A single 43-kD protein localized exclusively in the plasma membrane of pBK1-containing cells was detected (Fig. 4A). Likewise, immunoblots of proteins extracted from soybean nodules and roots (*16*) revealed an immunoreactive protein of 43 kD associated only with the PBM (Fig. 4B). The basis for the small discrepancy in size between the detected protein and the 39-kD polypeptide predicted from the cDNA sequence is unknown, but it could involve posttranslational modification (for example, by glycosylation). No such protein was identified in roots from which the nodules had been removed or in uninoculated roots (Fig. 4B). A protein of 50 kD was detected by the antiserum to GmSAT1 in total membranes from these roots but not in the PBM fraction. Because GmSAT1 mRNA was detected in nodules but not in uninfected roots (Fig. 3), the 50-kD protein probably is not encoded by *GmSAT1*.

Yeast 26972c cells containing pBK1 showed enhanced uptake of [^{14}C]methylammonium (MA; an ammonium analog) compared with control cells transformed with pYES3 vector alone (Fig. 5A). This is consistent with the

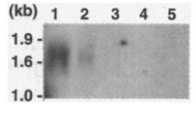

Fig. 3. Northern blot analysis (*12*) of 3 μg of poly$(A)^+$ RNA from nodulated and nonnodulated soybean tissues probed with antisense RNA synthesized from the full-length *GmSAT1* cDNA. Nodule (lane 1), roots after nodules were removed (lane 2), stem (lane 4), and leaf (lane 5) tissues were from nodulated plants; root tissue (lane 3) was from noninoculated nonnodulated NH_4NO_3 grown plants. Molecular size standards are indicated on the left. Results are representative of three independent determinations.

B. N. Kaiser, P. M. Finnegan, F. J. Bergersen, D. A. Day, M. K. Udvardi, Division of Biochemistry and Molecular Biology, The Australian National University, Canberra ACT 0200, Australia. S. D. Tyerman and L. F. Whitehead, Biology Department, Flinders, University of South Australia, GPO Box 2100, Adelaide 5001, Australia.

*To whom correspondence should be addressed.

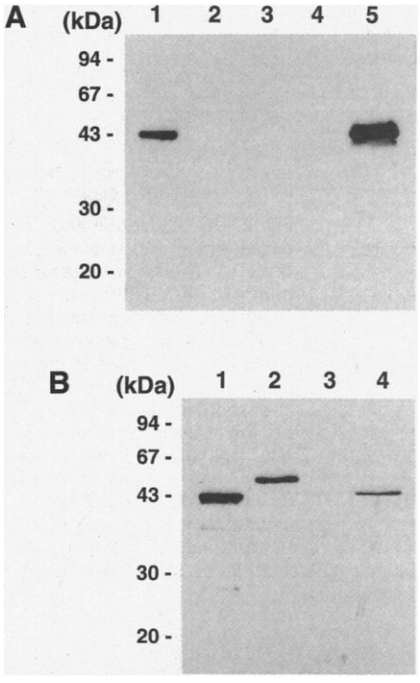

Fig. 4. Localization of GmSAT1 to the plasma membrane of yeast and the PBM of soybean root nodules (*16*). Antisera to GmSAT1 were used to probe SDS–polyacrylamide gel electrophoresis separated and electroblotted total soluble proteins from pBKHIS1-transformed *E. coli* (lane 1), soluble (lanes 2 and 3) and plasma membrane (lanes 4 and 5) proteins from yeast mutant 26972c transformed with either pYES3 (lanes 2 and 4) or pBK1 (lanes 3 and 5) (**A**), total soluble protein from pBKHIS1-transformed *E. coli* (lane 1), a total membrane fraction from 3.5-week-old nonnodulated roots (lane 2), and total soluble (lane 3) and PBM (lane 4) fractions of nodules (**B**). Molecular size markers are shown on the left. Fifteen micrograms of protein was loaded in each lane, except for *E. coli* extracts where 1 μg was loaded.

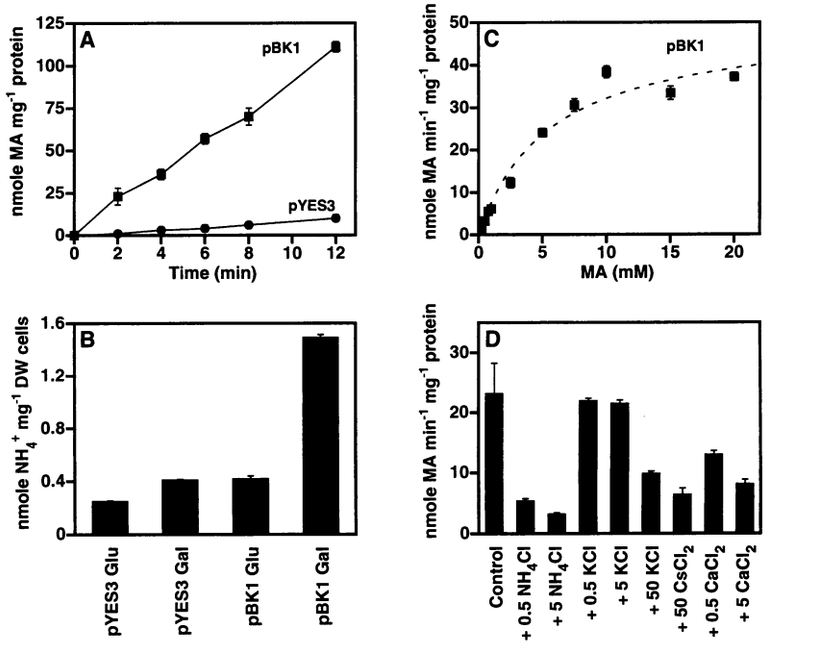

Fig. 5. Time course of [^{14}C]MA (*17*) (**A**) and $(^{15}NH_4)_2SO_4$ (**B**) uptake by mutant 26972c yeast cells transformed with either pBK1 or pYES3. Values are means ± SEM (n = 4). Uptake of [^{14}C]MA was measured by the filtration technique (*6*) and accumulation of $^{15}NH_4^+$ was estimated with a stable isotope analyzer (*17*). (**C**) Concentration dependence of [^{14}C]MA uptake by pBK1-transformed strain 26972c. Uptake rates of MA were determined over the first 2 min. The Michaelis-Menten equation was fitted to the data (dotted line, R^2 = 0.97). Values are means ± SEM (n = 4). (**D**) Inhibition of [^{14}C]MA uptake in pBK1-transformed cells by other cations. Competitor concentrations were 0.5, 5.0, or 50 mM, whereas MA remained constant at 0.5 mM. Values are means ± SEM (n = 4). Each panel presents typical data from one of four independent experiments.

inability of pBK1-containing cells to grow in the presence of the metabolic poison (Fig. 1C) (*17*). The concentration dependence of [^{14}C]MA uptake by cells expressing GmSAT1 showed saturation kinetics with an apparent K_m of 5.6 mM (Fig. 5C). This value is similar to that determined for the PBM NH_4^+ channels from soybean and pea (*3*). In contrast, the pYES3 transformed cells displayed a slow, linear uptake over the same MA concentrations (*13*). [^{14}C]MA uptake was inhibited severely by NH_4^+ at equimolar concentrations (Fig. 5D), consistent with GmSAT1 being an NH_4^+ transport protein. This was confirmed by experiments in which yeast was incubated with $^{15}NH_4^+$; only the cells under galactose induction and containing pBK1 showed substantial accumulation of ^{15}N (Fig. 5B). [^{14}C]MA uptake was inhibited by K^+ and Cs^+ at higher concentrations and also by Ca^{2+} in both the presence (*13*) and absence of Mg^{2+} (Fig. 5D).

The transport properties of pBK1-transformed yeast were further investigated by the patch-clamp method in the whole-cell configuration (*18*). Spheroplasts expressing GmSAT1 showed an inward current when bathed in 150 mM KCl with 175 mM KCl inside the pipette tip (Fig. 6, B and G). This current was not detected in wild-type yeast (*19*) or in 26972c cells transformed with cloning vector pYES3 (Fig. 6, C, D, and H). The reversal potential of inward current indicated that the current was carried by K^+ and not Cl^- (*20*). The inward currents had slow, time-dependent activation in response to increasingly negative voltage pulses (negative inside the cell) (Fig. 6, B and G) and were inhibited by the divalent cations Mg^{2+} and Ca^{2+} (Fig. 6, A and G). Inhibition of the cation inward currents by these divalent ions is consistent with the results observed during the MA-uptake experiments (Fig. 5D) and resembles the inhibition of NH_4^+ transport observed during patch-clamping of native PBM (*3*). All patches of the yeast spheroplasts showed a Ca^{2+}-sensitive outward current that was probably due to the action of the native yeast potassium outward rectifier (*19*) and not the result of GmSAT1 expression. In the presence of low NH_4^+ [1 mM, 2 mM (*20*), and 20 mM], currents were also measured across the plasma membrane of the GmSAT1-transformed yeast (Fig. 6, E and F). This NH_4^+ transport was severely reduced in the presence of Ca^{2+} (Fig. 6F) (replication of these results was hindered by disruption of the spheroplast membrane at this and higher NH_4^+ concentrations).

These data, together with those shown in Fig. 5, indicate that the expressed GmSAT1 protein catalyzes transport of monovalent cations, including NH_4^+, across the yeast plasma membrane. On the basis of the transport properties of GmSAT1 when expressed in yeast, and its localization on the PBM, we conclude that GmSAT1 is the previously identified PBM NH_4^+ channel (*3*). The lack of homology between the deduced amino acid sequence of GmSAT1 and known transport proteins in the databases is consistent with the unique properties of the PBM channel (*3*).

GmSAT1 has an unusual structure for a transport protein. The possibility of a single membrane-spanning helix may indicate that it forms homooligomers in the membrane to constitute an ion channel, as suggested for viral proteins with cation channel activity (*21*). In this context, the transmembrane helical region of GmSAT1 contains groups of polar amino acids that could be involved in pore formation in a homooligomer (*22*). Moreover, the helix-loop-helix motif could mediate dimerization. However, the overall structure of GmSAT1

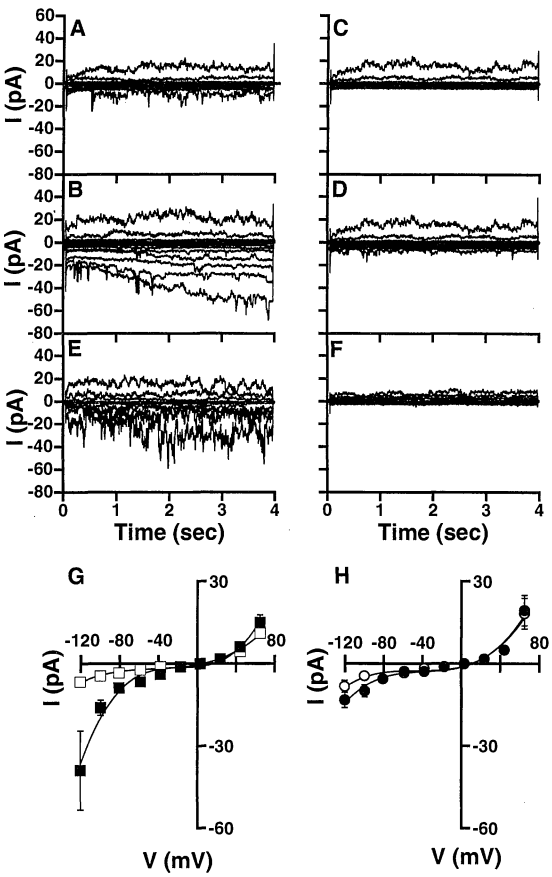

Fig. 6. K^+ currents across whole-cell patches of 26972c spheroplasts transformed with pBK1 (**A** and **B**) and pYES3 (**C** and **D**) in the presence [(A) and (C)] and absence [(B) and (D)] of Mg^{2+} and Ca^{2+}. NH_4^+ currents (**E** and **F**) in whole-cell patches of 26972c spheroplasts transformed with pBK1 in the presence of Mg^{2+} alone (E) or both Mg^{2+} and Ca^{2+} (F). Spheroplasts were made (*18*) according to a modification of (*19*). Bathing solutions: 150 mM KCl, 10 mM $CaCl_2$, 5 mM $MgCl_2$, galactose at 10 mg ml^{-1}, 5 mM tris-MES (pH 7.5); 20 mM NH_4Cl, 10 mM $CaCl_2$, 1 mM $MgCl_2$, galactose at 10 mg ml^{-1}, 5 mM Hepes-tris (pH 7.0). Pipette solution: 175 mM KCl, 4 mM K_2ATP, 0.1 mM $CaCl_2$, 5 mM $MgCl_2$, 1 mM EGTA (pH 7). All solutions were made up to 350 mosM with mannitol. Seal capacitances of whole-cell patches were between 3 and 6 pF. Currents were recorded from a series of voltage steps from +60 to −120 mV at 20-mV intervals. Currents were filtered at 100 Hz and digitized at 200 Hz. Current-voltage curves of K^+ currents (**G** and **H**) in whole-cell patches of 26972c spheroplasts transformed with pBK1 (G) or pYES3 (H) in the presence (open symbols) and absence (closed symbols) of divalent cations (10 mM Ca^{2+} and 5 mM Mg^{2+}). Values are means ± SEM (n = 8 or 9). Two-way analysis of variance showed that there was a significant difference in the behavior of inward K^+ currents of yeast transformed with pBK1 and pYES3 in the presence and absence of divalent cations (P = 0.05).

also resembles that of the cation channel Bcl-2, and in this protein it is the hydrophilic portion that confers channel activity (*23*). Elucidation of the mechanism of action of GmSAT1 will have implications for ion transport across membranes in general as well as for symbiotic nitrogen fixation.

The expression pattern of *GmSAT1* in soybean indicates that GmSAT1 plays a specialized role in symbiotic nitrogen fixation. In view of the biochemical, biophysical, and immunolocalization data presented here, we propose that this role is to transport NH_4^+ from the PBS to the cytoplasm of the infected plant cell.

References and Notes

1. E. Roth, K. Jeon, G. Stacey, in *Molecular Genetics of Plant-Microbe Interactions*, R. Palacios and D. P. S. Verma, Eds. (American Phytopathological Society, St. Paul, MN, 1988), p. 220.
2. M. K. Udvardi and D. A. Day, *Annu. Rev. Plant Physiol. Plant Mol. Biol.* **48**, 493 (1997).
3. S. D. Tyerman, L. F. Whitehead, D. A. Day, *Nature* **378**, 629 (1995); P. Mouritzen and L. Rosendahl, *Plant Physiol.* **115**, 519 (1997).
4. A. Marini, S. Soussi-Boudekou, S. Vissers, B. Andre, *Mol. Cell. Biol.* **17**, 4282 (1997).
5. A. Marini, S. Vissers, A. Urrestarazu, B. Andre, *EMBO J.* **13**, 3456 (1994).
6. O. Ninnemann, J. Jauniaux, W. B. Frommer, *ibid.*, p. 3464.
7. Total RNA was isolated from soybean nodules (*Glycine max* L. cv. Stevens inoculated with *Bradyrhizobium japonicum* USDA 110) by a guanidinium isothiocyanate, LiCl precipitation method [C. Puissant and L.-M. Houdebine, *Biotechniques* **8**, 148 (1990)]. Poly(A)$^+$ RNA was selected by using oligo(dT)-cellulose spin columns (Pharmacia). Three micrograms of poly(A)$^+$ RNA was converted to double-stranded cDNA with a commercial kit (Gibco-BRL) and ligated (*10*) into *Sal* I–*Not* I digested pYES3 (*8*). The library was amplified in *E. coli* strain DH10B (*10*) before transformation [R. H. Schiestl and R. D. Gietz, *Curr. Genet.* **16**, 339 (1989)] into *S. cerevisiae* strain 26972c (*mep1mep2ura3*) (*4*).
8. F. W. Smith, P. M. Ealing, M. J. Hawkesford, D. T. Clarkson, *Proc. Natl. Acad. Sci. U.S.A.* **92**, 9373 (1995).
9. Mutant 26972c (*4*) cells transformed with the soybean nodule cDNA library (*7*) were plated onto yeast minimal medium [F. Ramos and J. Wiame, *Eur. J. Biochem.* **94**, 409 (1979)] deficient in uracil and supplemented with 1 mM $(NH_4)_2SO_4$ and galactose at 10 mg ml^{-1}. After growth at 28°C, surviving colonies were transferred in duplicate onto solid minimal medium supplemented with 1 mM $(NH_4)_2SO_4$ and galactose or glucose at 10 mg ml^{-1}. Colonies that grew in the presence of galactose but not glucose were analyzed further to confirm that the galactose-dependent growth at low NH_4^+ concentrations was plasmid mediated. Transformants displaying linkage between uracil independence, galactose-inducible, glucose-repressible growth on 2 mM NH_4^+ and nonviability on 0.1 M MA-containing media were selected. Plasmids contained in these transformants were isolated and retransformed into 26972c to reconfirm their ability to mediate phenotypic rescue. Transformants were maintained on minimal medium containing 0.1 M MA, 0.1% L-proline, and glucose at 10 mg ml^{-1}.
10. J. Sambrook, E. F. Fritsch, T. Maniatis, *Molecular Cloning: A Laboratory Manual* (Cold Spring Harbor Laboratory Press, Cold Spring Harbor, NY, 1989).
11. J. Kyte and R. F. Doolittle, *J. Mol. Biol.* **157**, 105 (1982); B. Rost, R. Casadio, P. Fariselli, C. Sander, *Prot. Sci.* **4**, 521 (1995).
12. Soybeans were planted in river sand and grown in a glass house at 20° to 30°C. Some plants were inoculated with *B. japonicum* USDA 110 and irrigated with nutrient medium lacking nitrogen [A. C. Delves *et al.*, *Plant Physiol.* **82**, 588 (1986)], and others were not inoculated but were irrigated with nutrient solution containing 5 mM NH_4NO_3. Four weeks after planting, tissues were harvested and frozen immediately in liquid N_2. After total RNA extraction [C. Puissant and L. Houdebine, *Biotechniques* **8**, 148 (1990)], poly(A)$^+$ RNA was isolated with Oligotex oligo(dT) matrix (Qiagen), separated on agarose gels containing formaldehyde (*10*), blotted by capillary action to Hybond-N$^+$ nylon membrane (Amersham), and hybridized with full-length digoxigenin-labeled (Boehringer Mannheim) *GmSAT1* antisense RNA. Membranes were washed at high stringency [68°C for 30 min in 0.1× SSC (*10*) containing 1% (w/v) SDS] before autoradiography.
13. B. N. Kaiser, unpublished data.
14. A 1.4-kb Bam HI–Xho I fragment of pBK1, harboring all but the 21 NH_2-terminal amino acids of the *GmSAT1* open reading frame, was subcloned in-frame with the translational start of the *E. coli* expression vector pTrcHisB (Invitrogen) to generate pBKHIS1. To remove the hydrophobic COOH-terminus from GmSAT1, pBKHIS1 was digested with Hind III and religated to produce pBK1HIS2, which encodes amino acid residues 22 to 204 of GmSAT1 in-frame with both the initiation and termination codons of the expression vector. To produce fusion proteins, transformed *E. coli* DH10B cells were first grown at 37°C in LB medium (*10*) containing ampicillin at 125 μg ml^{-1} to an OD_{600} of 0.5. Expression of the fusion protein was induced by adding 1 mM isopropyl β-D-thiogalactopyranoside (IPTG) and incubating at 37°C for a further 3 hours. Cells were harvested, resuspended in lysis buffer [8 M urea, 50 mM NaH_2PO_4, 200 mM NaCl, 1.5 mM imidazole (pH 8.0)], and disrupted by six cycles of freezing and thawing followed by sonication for six 30-s periods, with 1 min of cooling on ice between each sonication step. Insoluble protein and cell debris were removed by centrifugation at 10,000*g* for 30 min. Protein blot analysis using an antibody to His_6 (Qiagen) demonstrated that soluble *E. coli* DH10B cell fractions from pBK1HIS1 or pBK1HIS2 transformed cells contained IPTG-inducible immunoreactive proteins of 42 and 26 kD, respectively (results not shown). Approximately 3 kD of each of these fusion proteins is encoded by the pTrcHisB vector.
15. The His_6-tagged portion of GmSAT1 encoded by pBK1HIS2 was purified from a 500-ml culture by immobilized metal affinity chromatography according to the supplier's protocol (Clonetech). Eluted proteins were concentrated by trichloroacetic acid precipitation and resuspended in urea-containing elution buffer to a final concentration of 1 mg ml^{-1}. Antiserum was generated by standard techniques [E. Harlow and D. Lane, *Anitbodies: A Laboratory Manual* (Cold Spring Harbor Laboratory Press, Cold Spring Harbor, NY, 1988)] with 200 μg of fusion protein administered per injection.
16. Crude plasma membrane was prepared [F. Supeck, L. Supeckova, H. Nelson, N. Nelson. *Proc. Natl. Acad. Sci. U.S.A.* **93**, 5105 (1996)] from mechanically disrupted [J. Dufour, A. Amory, A. Goffeau. *Methods Enzymol.* **157**, 513 (1988)] yeast 26972c cells containing either pBK1 or pYES3 grown at 28°C for 24 hours in minimal medium containing galactose at 20 mg ml^{-1} and 1 or 10 mM NH_4Cl, respectively. Plasma membrane was purified further by fractionation on a discontinuous 43% to 53% sucrose gradient (R. Serrano, *ibid.*, p. 533). Root membrane and soluble nodule protein fractions were prepared from 3.5-week-old nonnodulated and nodulated soybean plants, respectively, after homogenization in extraction buffer [25 mM MES-KOH (pH 7.0), 350 mM mannitol, 3 mM $MgSO_4$, 1 mM phenylmethylsulfonyl fluoride (PMSF)] with a mortar and pestle. The homogenates were filtered through four layers of Miracloth (Calbiochem) and centrifuged at 20,000*g*

for 15 min. The supernatants were centrifuged at 125,000*g* for 1 hour. The total membrane pellet from roots was resuspended in solubilization buffer [50 mM KPO_4 (pH 6.3), 20% (v/v) glycerol, 1 mM $MgCl_2$, 1 mM PMSF] and the soluble (supernatant) fraction from nodules was concentrated by ammonium acetate–methanol precipitation. PBM was obtained from symbiosomes isolated from the nodules of 3.5-week-old soybean plants [D. A. Day and M. K. Udvardi. *Aust. J. Plant. Physiol.* **16**, 69 (1989)]. PBM purity was verified routinely by microscopy and enzymatic assays (NADH-oxidase as a mitochondrial marker, NADPH-cytochrome c reductase as a plasma membrane marker, carotene as a plastid membrane marker) as described [L-J. OuYang, M. K. Udvardi, D. A. Day, *Planta* **182**, 437 (1990)]. PBM proteins were extracted from the membrane with phenol [W. J. Hurkman and C. K. Tanaka, *Plant Physiol.* **81**, 802 (1986)]. Proteins were separated by SDS–polyacrylamide gel electrophoresis [U. K. Laemmli, *Nature* **227**, 680 (1970)] and transferred to Hybond C-extra nitrocellulose membranes (Amersham) with a semidry blotter (Millipore). Immunoblots were probed with antiserum to GmSAT1 at a dilution of 1:5000. Immunoreactive proteins were visualized by chemiluminescence with a commercially available kit (Boehringer Mannheim).

17. [^{14}C]MA uptake and cation competition experiments in yeast strain 26972c containing either pBK1 or the pYES3 cloning vector alone were performed as described in (*6*) after growth in liquid minimal medium supplemented with galactose at 10 mg ml^{-1} and 1 or 3 mM $(NH_4)_2SO_4$, respectively. $^{15}NH_4^+$ uptake was measured on cells grown initially on minimal medium (0.1 M MA, 0.1% L-proline, and glucose at 10 mg ml^{-1}), harvested, washed twice in sterile distilled H_2O, and then added to galactose or glucose (10 mg ml^{-1}) minimal medium containing 1.5% labeled 0.5 mM $(^{15}NH_4)_2SO_4$ to a final OD_{600} of 0.5. Cells were grown for 24 hours at 28°C, harvested, and washed in sterile distilled H_2O. Samples of cells were dried in tin foil capsules (15.6 to 18.8 mg dry weight) and analyzed for total N and ^{15}N with an ANCA-SL 2020 stable isotope analyzer (Europa Scientific, Crewe, UK).
18. Yeast cells containing either pBK1 or the pYES3 cloning vector were grown in supplemented minimal medium (*17*) and spheroplasts were produced (*19*) by digestion of cells with lyticase at 2 mg ml^{-1} (Sigma) instead of a mixture of zymolase and glucoronidase.
19. A. Bertl, J. A. Anderson, C. L. Slayman, R. F. Gaber, *Proc. Natl. Acad. Sci. U.S.A.* **92**, 2701 (1995).
20. B. N. Kaiser, L. F. Whitehead, S. D. Tyerman, unpublished data.
21. U. Schubert *et al.*, *FEBS Lett.* **398**, 12 (1996); S. C. Piller, G. D. Ewart, A. Premkumar, G. B. Cox, P. W. Gage, *Proc. Natl. Acad. Sci. U.S.A.* **93**, 111 (1996).
22. J. Devereux, P. Haeberli, O. Smithies, *Nucleic Acids Res.* **12**, 387 (1984).
23. A. J. Minn *et al.*, *Nature* **385**, 353 (1997).
24. We thank G. Turner, CSIRO Plant Industry, Canberra, for ^{15}N analysis; S. Howitt for her assistance with sequence analysis; M. Ludwig for helpful discussions; and R. Thomson for assistance with the membrane preparations. Supported by Australian Research Council grants to D.A.D., S.D.T., and M.K.U. and an Australian National University postgraduate scholarship from the Cooperative Research Centre for Plant Science to B.N.K.

10 April 1998; accepted 9 July 1998